Copyright © 2008 American Scientific Publishers
All rights reserved
Printed in the United States of America

Journal of Nanoscience and Nanotechnology
Vol. 8, 5640–5645, 2008

Scanning Probe Oxidation Lithography on Ta Thin Films

Salih Okur*, Serkan Büyükköse, and Suleyman Tari

Department of Physics, İzmir Institute of Technology, Urla, 35430, İzmir, Turkey

A Semi-Contact Scanning Probe Lithography Technique (SC-SPL) has been applied to create nano-oxide patterns on Ta thin films grown by DC magnetron sputtering method on SiO_2/Si substrates. The height and linewidth profiles of nano-oxide lines created by a conductive AFM tip on Ta film surfaces were measured as a function of applied voltage, oxidation time, humidity, and tip apex curvature. The AFM surface measurements show that the height of the oxides increases linearly with increasing voltage; but there was no oxide growth, when less than 4 V was applied even at 85% relative humidity. Electrical measurements were performed and the resistivities of the TaO_x layer and Ta film were obtained as 5.76×10^8 and 1.4×10^{-5} Ohm-cm, respectively.

Keywords: Scanning Probe Lithography, Nano-Oxidation, Tantalum Thin Film, Tantalum Oxide, Insulating Thin Films, Electrical Resistivity, Dielectric Thin Films.

RESEARCH ARTICLE

1. INTRODUCTION

Creation of smaller electronic devices enforces the use of materials with higher dielectric constants (κ) than that of SiO_2 ($\kappa = 3.9$).[1] Tantalum pentoxide (Ta_2O_5), an electrical insulator with dielectric constant $\kappa > 26$, is one of the best candidates to be used as a gate barrier instead of SiO_2 in field effect transistors and in DRAM capacitors.[2,3] Several techniques such as electron beam gun evaporation,[4] and reactive pulsed direct-current magnetron sputtering[5] have been used to fabricate highly insulating tantalum pentoxide capacitor films. Tip-induced Scanning Probe Lithography (SPL) technique has been used to create nanostructures below 100 nm[6] on semiconductors[7–9] and metals surfaces such as chromium,[10] titanium,[11–12] niobium[13] and on tantalum films in contact mode.[14–15] There are some successful applications of nanoelectronic devices fabricated using SPL reported in the literature, such as field effect transistors (FETs),[16–19] Josephson junctions[20] and superconducting quantum interference devices (SQUID).[21]

In the SC-SPL technique, a bias voltage between an oscillating sharp tip and a conductive sample generates an intense electric field (10^9 V/m) at the apex of an AFM tip. This field is comparable to the effective field on electrons around atoms. The tip-sample spacing is maintained with an SPM feedback loop to allow controlled patterning with continuous and uniform features on metallic surfaces. A high electric field between tip and sample leads to decomposition of the water layer ($2H_2O = 2(HO)^- + H_2^+$),[22–23] and accumulation of energetic hydroxyl ions being accelerated to the Ta surface, establishing a nanosize electrochemical process in ambient conditions. The oxidation rate can be controlled by growth parameters such as amplitude of applied voltage, lithography time, humidity, tip-sample separation, substrate temperature and substrate property.[21,24–25] One of the possible electrochemical reactions on a Ta film under an oscillating electric field and within a controlled humidity environment can be described by the following electrochemical reaction:

$$4Ta^+ + 10x(HO)^- \rightarrow 2Ta_2O_{5x} + 5xH_2 \quad (1)$$

Tantalum oxide (Ta_2O_{5x}) is one of the most likely stable oxide phases to be formed in this process and is suggested in the previous works.[14–15] But recent SPL and EDS study on Si substrate shows that anodic oxidation process increases the native oxide composition stoichiometry. The EDS spectrum taken from the tip induced SiO_x patterns on native SiO_2 on Si substrate shows that the O/Si ratio is greater than two ($x > 2$).[26–27]

In this work, we report the tantalum oxide nanopatterns created using scanning probe lithography technique in semi-contact (tapping) mode (SC-SPL). Ta oxide patterns with linewidths as small as 75 nm were successfully produced. Spreading surface resistance image (SRI) and local resistivity of 2.3 nm thick TaO_x fabricated with SPL technique on a fresh Ta film produced with DC magnetron sputtering method were measured with a DLC coated conductive AFM tip in contact mode.

*Author to whom correspondence should be addressed.

1533-4880/2008/8/5640/006 doi:10.1166/jnn.2008.324

2. EXPERIMENTAL DETAILS

A thin Ta film with 20 nm thickness was deposited on thermally oxidized SiO_2 (~1 μm) on Si(100) wafers (purchased from Si-Mat) by DC magnetron sputtering. SC-SPL local oxidation experiments were performed using a commercial Scanning Probe Microscopy (SPM) instrument (Solver Pro 7 from NT-MDT, Russia) with a conductive diamond like carbon coated tip (DLC tip from the same company) with a curvature of 75 nm. The RMS surface roughness of the Ta films was measured as 0.12 nm. A positive bias voltage between 1 V and 10 V was applied to the Ta film while the tip at a distance of 10 nm from the Ta film was grounded. The tip with an oscillating frequency of 691 kHz is at lower potential with respect to the counter electrode on the Ta film. The experiments were carried out in an environmental AFM chamber to control relative humidity between 5%–85%.

3. RESULTS AND DISCUSSION

Figures 1(a) and (b) show the 2D AFM surface image and height profile of TaO_x nano-patterns for various oxidation voltage durations ranging from 1 ms to 210 ms. TaO_x line patterns were created with constant 10 V tip-sample voltage under 85% relative humidity at 23 °C substrate temperature. All of the obtained oxide patterns are homogenous and showed significant change in height depending on voltage duration. The height of the oxide patterns increased from 2 nm to 4.2 nm with increasing oxidation time between 1 ms and 210 ms.

There are several phenomenological models[7,23,27–30] to predict the oxide thickness $h(t)$ as a function of time t and voltage V using the potential distribution in the oxide layer. Among these models, the empirical power law to describe oxide growth kinetics as a power of pulse duration,[31–32] the logarithmic function of applied voltage duration, assuming the electric field, $E = V/h$; where V is the applied voltage and h is the tip-sample separation,[7] and the inverse exponential growth function of time,[23,27] have been used to fit the anodic oxidation data obtained by SPL experiment. Recently, Orians et al.[31] have proposed a numerical model including the influence of the space charge due to ions trapped near the substrate/oxide interface to predict features of oxide growth to include operating and material parameters on the thickness of the oxide, the electric field, and ion concentration in the system; but their results resemble the power law introduced by Teuschler.[29] We have used the inverse exponential growth model formulated with the following equations to fit our TaO_x data;

$$\frac{dh}{dt} = \left(\frac{h_0}{\tau}\right)e^{-t/\tau} \quad (2)$$

$$h = h_m - h_0 e^{-t/\tau} \quad (3)$$

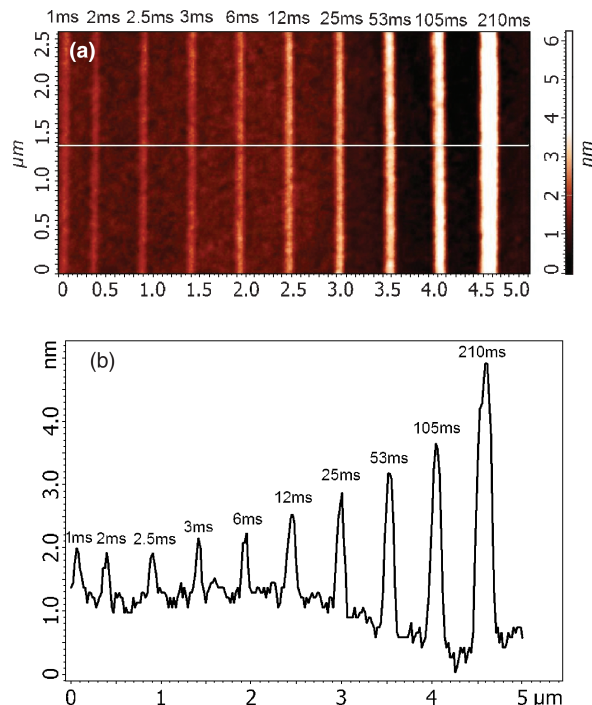

Fig. 1. (a) The 2D AFM image and (b) the height profile of tantalum oxide nano-patterns for various sample voltage duration ranging from 1 ms to 210 ms (oxidation voltage: $V = 10$ V, humidity RH = 85%, temperature $T = 23$ °C).

where h and t represent the oxide height and applied voltage pulse duration, h_m, and h_0 are the initial constants, and τ is the curve-fitted time constant, respectively. Equation (3) shows time dependence of the oxide height. Figure 2 shows the effect of applied tip-sample voltage duration on oxide height. For the exponential growth function of the oxide line protrusions on the fresh Ta layer, the best fit parameters are obtained as $h_m = 4.4$ nm, $h_0 = 1.98$ nm, $\tau = 88.5$ ms. From the beginning up to time constant, $\tau = 88.5$ ms, the oxidation process is faster due to the low dielectric barrier of the water meniscus on the

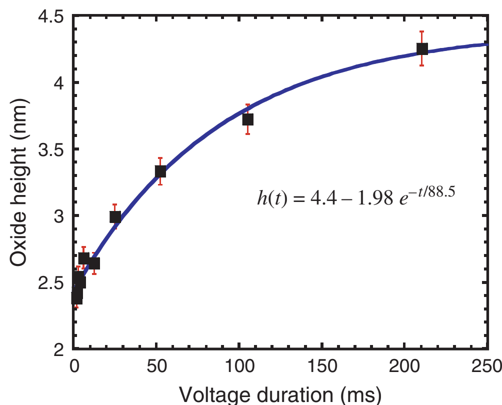

Fig. 2. The effect of sample voltage duration on Ta oxide growth (oxidation voltage $V = 10$ V, relative humidity RH = 85%, temperature $T = 25$ °C).

surface. Then, the oxidation process starts to saturate to $h_m = 4.4$ nm due to TaO_x dielectric material growth underneath the tip and increasing the space charge accumulation due to ions trapped near the substrate/oxide interface.[31]

The oxide growth rate is very sensitive to the applied voltage between the conductive tip and bare Ta surface, since the electric field is an important experimental parameter in a local electrochemical process. Figures 3(a) and (b) show the 3D AFM image and the height profile of TaO_x lines, respectively. The oxide height and linewidth dependences of TaO_x nano-patterns on various tip-sample voltages applied between 1 V and 10 V, under 85% relative humidity at 25 °C are given in Figure 3(c). Both the oxide height and the oxide linewidth increase linearly with

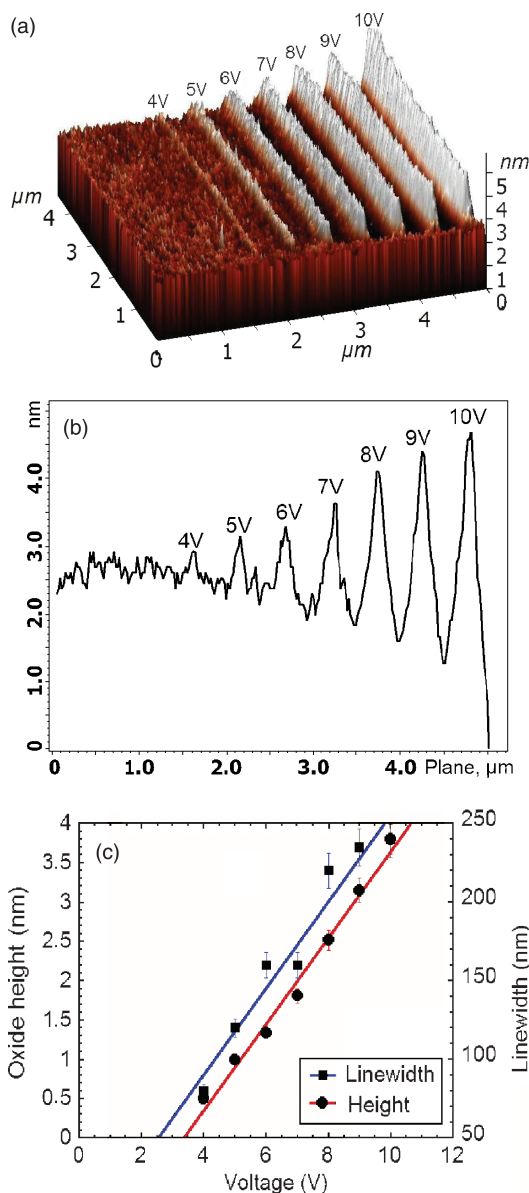

Fig. 3. (a) The 3D AFM image, (b) the height profile, (c) oxide height (left) and linewidth (right) profile of TaO_x nano-patterns for various oxidation voltages under 85% relative humidity at 25 °C.

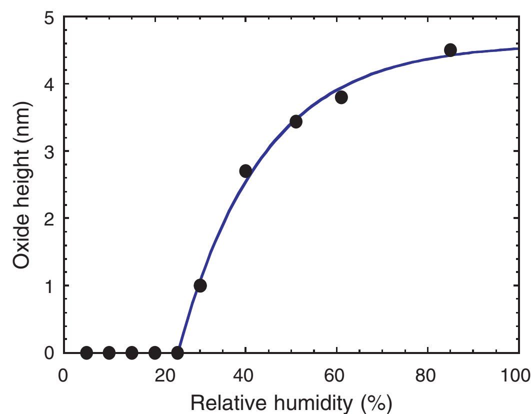

Fig. 4. The effect of relative humidity on Ta oxide growth under 10 V oxidation voltage applied for 210 ms at 25 °C substrate temperature.

increasing oxidation voltage. It was also seen that there is no grown oxide less than 4 V even at 85% relative humidity. This means that the oxidation time for the applied voltage is not enough for a measurable oxide protrusion height for our SPM system.[33–35]

Relative humidity is another effective parameter as a source of water meniscus bridge to establish the local electrochemical process between the conductive tip and the Ta metal thin film surface. The effect of relative humidity on TaO_x for 10 V tip-sample voltage for 210 ms pulse duration at 25 °C substrate temperature is shown in Figure 4. Oxidation starts around 25% relative humidity (RH) and increases with increasing RH and then starts to saturate around 70%. This means that relative humidity less than

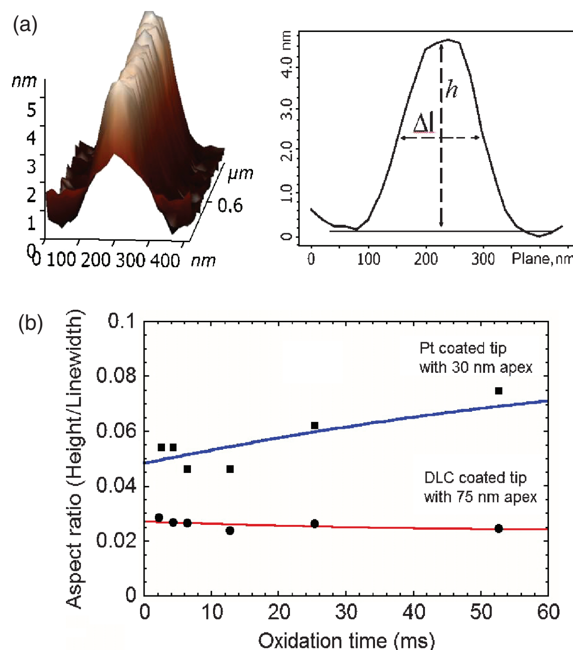

Fig. 5. (a) The oxide height and the average full width at half maximum (FWHM) of the oxide line protrusions, (b) effect of oxidation time on aspect ratio for AFM tips with two different apex curvatures.

RESEARCH ARTICLE

25% is not enough to set a water meniscus bridge along 10 nm tip sample separation to start the local electrochemical process.[33–35]

We also measured the effect of oxidation time and tip apex curvature on the aspect ratio (the ratio of oxide height and the average full width at half maximum (FWHM) of oxide line protrusion) as depicted in Figure 5(a). Aspect ratio versus oxidation time for AFM tips with two different apex curvatures is shown in Figure 5(b). The aspect ratio of the Pt coated tips with 30 nm apex curvature is approximately twice that of the DLC coated tip with 75 nm apex curvature. This means sharper tips produce thinner patterns, which affects consequently the resolution of SPM nanolithography. There is a slight increase in the aspect ratio for the DLC coated tips, while the aspect ratio is approximately constant for the Pt coated tips. Compared to previous works on Ta thin films done in contact mode SPL,[14–15] higher TaO_x growth rate and aspect ratio are obtained in SC-SPL as a result of space charge minimization by varying electric field due to oscillating AFM tip. Recent study with a shorter duration time of pulsed voltage has proved to be able to fabricate significantly improved high aspect ratio oxide compared to the conventional AFM anodization lithography process using continuous bias.[36]

For electrical characterization, a 1×1 μm^2 TaO_x layer with oxide height of 2.3 nm was formed on a Ta film to measure the electrical properties of TaO_x. The 3D surface topography and the spreading surface resistance image (SRI) of the TaO_x layer on this Ta film are shown in Figures 6(a) and (b) respectively. Two terminal electrical measurements were done in contact mode allowing the AFM tip to touch the oxide layer or Ta surface. The distance between the conductive tip and counter electrode was kept at 5 mm. Around 15 nA current difference as the contrast of the SRI image between Ta and the TaO_x surface is seen in Figure 6(b). Darker contrast shows higher resistive areas on the picture. This means that the TaO_x dielectric material should have more resistance compare to Ta surface. To measure and compare the resistivities of the TaO_x layer and Ta film (inlet), I–V curves have been taken with the same DLC coated conductive AFM tip as shown in Figure 7. Resistances obtained from I–V curves were 3×10^{12} Ω and 5×10^5 Ω for the bare TaO_x layer and the Ta film for linear regions, respectively. The corresponding resistivities were calculated from $\rho = RA/l$, where R is the resistance, A is the cross-sectional area of the tip apex (75 nm) and l (5 mm) is the distance between the tip and the counter electrode. The transverse resistivity

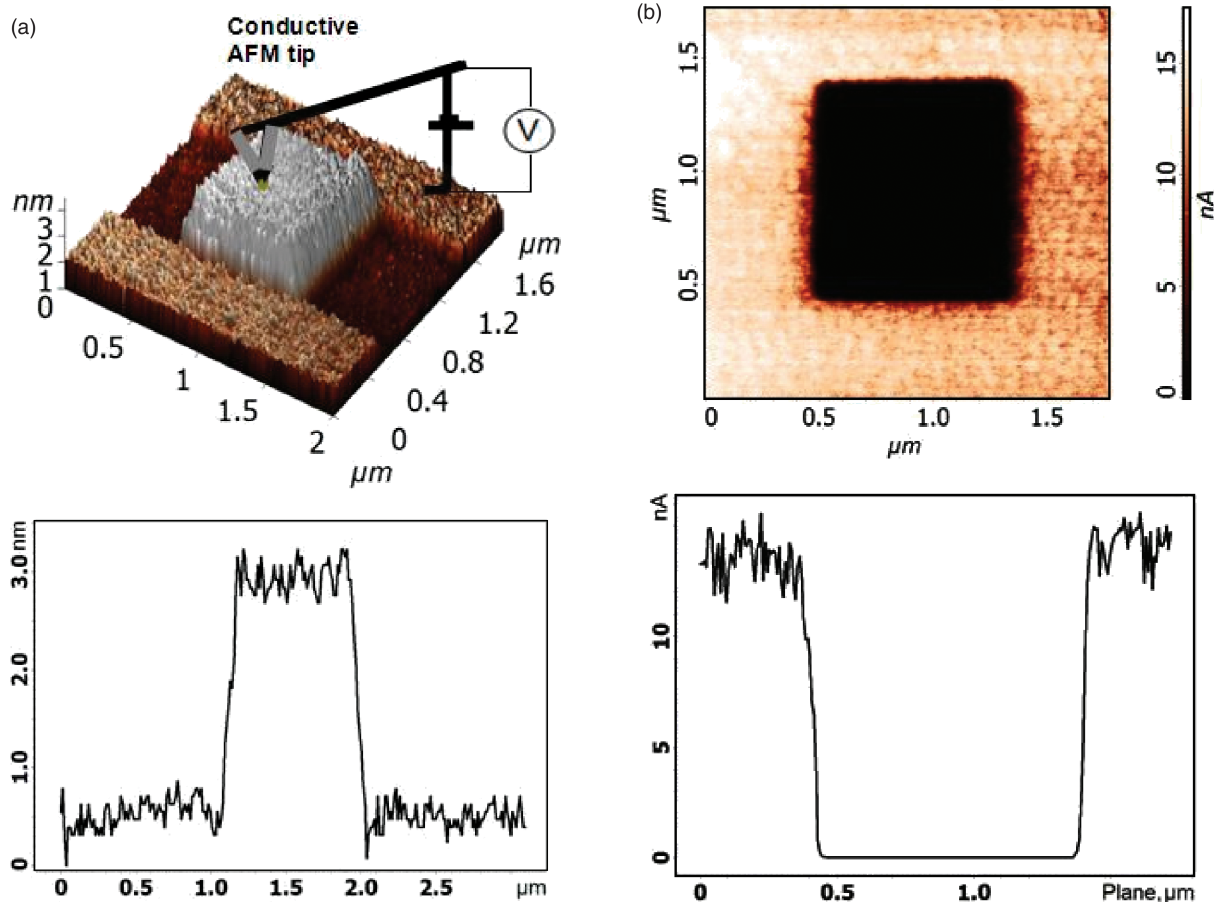

Fig. 6. (a) The 3D surface topography and (b) the spreading surface resistance image of Ta thin film after the local oxidation.

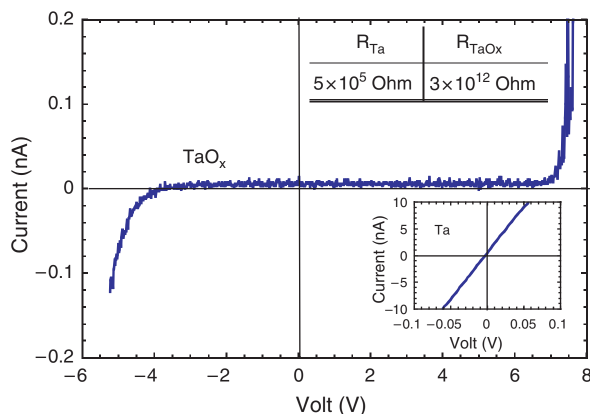

Fig. 7. *I–V* characteristics of the TaO_x layer and the bare Ta film (inset).

of the TaO_x layer is measured as 5.76×10^8 Ohm-cm and the longitudinal resistivity of Ta film is measured as 1.4×10^{-5} Ohm-cm. The resistivity ratio of TaO_x and Ta is obtained as 4.02×10^{13}. The resistivity of the TaO_x layer is low compared to the resistivity (4.8×10^{13} Ohm-cm) of a 10 nm thick Ta_2O_5 film obtained by dry O_3 annealing at 450 °C as measured by the Moon group.[37] This may be due to possible leakage (tunneling) currents caused from defects and charge traps through the 2.3 nm thin tantalum oxide. More detailed studies such as EDS, XPS and capacitance measurements are needed to characterize structural and electronic properties of tantalum oxide produced with tip induced SPL techniques.

4. CONCLUSION

In summary, tip induced local oxidation parameters of TaO_x fabricated by SPL technique were investigated by applying positive bias voltage to Ta thin film surface and varying relative humidity at constant substrate temperature. The oxide height and FWHM were found to increase with increasing voltage amplitude and duration. It was found that tip voltage strength and relative humidity have the most influence on oxide growth rate. There was no measurable oxide growth for voltages less than 4 V and relative humidity values less than 25% due to insufficient environmental conditions to set the local electrochemical process between tip and Ta substrate. The aspect ratio between oxide height and FWHM of oxide line protrusions depends on the apex curvatures of the conductive AFM tips and does not change significantly with oxidation time. Two terminal electrical measurements were performed with a conductive AFM tip in contact mode and the resistivities of the TaO_x layer and the Ta film were obtained as 5.76×10^8 Ohm-cm and 1.4×10^{-5} Ohm-cm in the linear *I–V* regions, respectively.

Acknowledgments: This research was partially supported by DPT (State Planning Organization of Turkey) under project number DPT2003K120390, IYTE research project numbers 2004İYTE22 and 2006İYTE21.

References and Notes

1. G. D. Wilk, R. M. Wallace, and J. M. Anthony, *Appl. Phys. Rev.* 89, 5243 **(2001)**.
2. J. K. Schaeffer, Dissertation Degree of Doctor of Philosophy, The University of Texas at Austin **(2004)**.
3. Y. Kang, P. M. Lenahan, and J. Conley, *Appl. Phys. Lett.* 83, 3407 **(2003)**.
4. V. Mikhelashvili and G. Eisenstein, *Appl. Phys. Lett.* 75, 2836 **(1999)**.
5. J. Kim, M. C. Nielsen, E. J. Rymaszewski, and T. M. Lu, *J. Appl. Phys.* 87, 1448 **(2000)**.
6. H. T. Soh, K. W. Guarini, and C. F. Quate, Scanning Probe Lithography, Kluwer, Boston **(2001)**.
7. Ph. Avouris, T. Hertel, and R. Martel, *Appl. Phys. Lett.* 71, 285 **(1997)**.
8. M. Tello, F. García, and R. García, *J. Appl. Phys.* 92, 4075 **(2002)**.
9. E. S. Snow and P. M. Campbell, *Appl. Phys. Lett.* 64, 1932 **(1994)**.
10. D. Wang, L. Tsau, K. L. Wang, and P. Chow, *Appl. Phys. Lett.* 67, 1295 **(1995)**.
11. B. Irmer, M. Kehrle, and J. P. Kotthaus, *Appl. Phys. Lett.* 71, 1733 **(1997)**.
12. S. Lemeshko, S. Gavrilov, V. Shevyakov, V. Roschin, and R. Solomatenko, *Nanotechnology* 12, 273 **(2001)**.
13. J. Shiracashi, K. Matsumoto, N. Miura, and M. Konagai, *Jpn. J. Appl. Phys.* 36, L1257 **(1997)**.
14. Y. H. Kim, J. Zhao, and K. Uosaki, *J. Appl. Phys.* 94, 7733 **(2003)**.
15. S. Lee, H. Lee, D. H. Lee, B.-J. Park, and G. Y. Yeom, *Mol. Cryst. Liq. Cryst.* 445, 115 **(2006)**.
16. P. M. Campbell, E. S. Snow, and P. J. McMarr, *Appl. Phys. Lett.* 66, 1388 **(1995)**.
17. I. Pallecchi, L. Pellegrino, E. Bellingeri, A. S. Siri, and D. Marre, *J. Appl. Phys.* 95, 8079 **(2004)**.
18. E. S. Snow, P. M. Campbell, R. W. Rendell, F. A. Buot, D. Park, C. R. K. Marrian, and R. Magno, *Appl. Phys. Lett.* 72, 3071 **(1998)**.
19. L. Pellegrino, I. Pallecchi, D. Marre, E. Bellingeri, and A. S. Siri, *Appl. Phys. Lett.* 81, 3849 **(2002)**.
20. V. Bouchiat, M. Faucher, C. Thirion, W. Wernsdorfer, T. Fournier, and B. Pannetier, *Appl. Phys. Lett.* 79, 123 **(2001)**.
21. I. Song, B. M. Kim, and G. Park, *Appl. Phys. Lett.* 76, 601 **(2000)**.
22. E. S. Snow and P. M. Campbell, *Science* 270, 1639 **(1995)**.
23. Y. R. Ma, C. Yu, Y. D. Yao, Y. Liou, and S. F. Lee, *Phys. Rev. B* 64, 195324 **(2001)**.
24. R. W. Li, T. Kanki, H. A. Tohyama, J. Zhang, H. Tanaka, A. Takagi, T. Matsumoto, and T. Kawai, *J. Appl. Phys.* 95, 7091 **(2004)**.
25. W. Lee, E. R. Kim, and H. Lee, *Langmuir* 18, 8375 **(2002)**.
26. H. Sugimura, T. Uchida, N. Kitamura, and H. Masuhara, *Jpn. J. Appl. Phys.* 32, L553 **(1993)**.
27. Y. S. Lu, H. I. Wu, S. Y. Wu, and Y. R. Ma, *Surf. Sci.* 601, 3788 **(2007)**.
28. S. Konsek, R. Coope, T. Pearsall, and T. Tiedje, *Appl. Phys. Lett.* 70, 1846 **(1997)**.
29. A. Orians, C. B. Clemons, D. Golovaty, and G. W. Young, *Surf. Sci.* 600, 3297 **(2006)**.
30. R. Garcia and M. Calleja, *Appl. Phys. Lett.* 72, 2295 **(1998)**.
31. T. Teuschler, K. Mahr, S. Miyazaki, M. Hundhausen, and L. Ley, *Appl. Phys. Lett.* 67, 3144 **(1995)**.

32. J. A. Dagata, F. Perez-Murano, G. Abadal, K. Morimoto, T. Inoue, J. Itoh, and H. Yokoyama, *Appl. Phys. Lett.* 76, 2710 **(2000)**.
33. M. Calleja and R. Garcia, *Appl. Phys. Lett.* 76, 3427 **(2000)**.
34. R. Garcia, M. Calleja, and H. Rohrer, *J. Appl. Phys.* 86, 1898 **(1999)**.
35. M. Tello and R. Garcia, *Appl. Phys. Lett.* 79, 424 **(2001)**.
36. S. Bae, C. Han, M. S. Kim, C. C. Chung, and H. Lee, *Nanotechnology* 16, 2082 **(2005)**.
37. B. K. Moon, C. Isobe, and J. Aoyama, *J. Appl. Phys.* 85, 1731 **(1999)**.

Received: 7 October 2007. Accepted: 24 January 2008.

RESEARCH ARTICLE